

SDSS J160531.84+174826.1: A Dwarf Disk Galaxy With An Intermediate-Mass Black Hole

Xiaobo Dong^{1,2}, Tinggui Wang^{1,2}, Weimin Yuan³, Hongguang Shan³, Hongyan Zhou^{1,2,4},
Lulu Fan^{1,2}, Liming Dou³, Huiyuan Wang^{1,2}, Junxian Wang^{1,2}, and Honglin Lu^{1,2}

xbdong, twang@ustc.edu.cn; wmy@ynao.ac.cn

ABSTRACT

We report the discovery of a dwarf Seyfert 1 active galactic nucleus (AGN) with a candidate intermediate-mass black hole hosted by the dwarf galaxy SDSS J160531.84+174826.1 at $z = 0.032$. A broad component of the $H\alpha$ line with $\text{FWHM}=781\text{km s}^{-1}$ is detected in its optical spectrum, and a bright, point-like nucleus is evident from a HST imaging observation. Non-thermal X-ray emission is also detected from the nucleus. The black hole mass, as estimated from the luminosity and width of the broad $H\alpha$ component, is about $7 \times 10^4 M_\odot$. The host galaxy appears to be a disk galaxy with a boxy bulge or nuclear bar; with an absolute magnitude of $M_R = -17.8$, it is among the least luminous host galaxies ever identified for a Seyfert 1.

Subject headings: galaxies: active — galaxies: dwarf — galaxies: individual (SDSS J160531.84+174826.1) — galaxies: nuclei — galaxies: Seyfert

1. Introduction

Supermassive black holes (SMBHs) with masses $M_{BH} \gtrsim 10^6 M_\odot$ have been convincingly inferred to be present in the centers of nearby galaxies (see Kormendy 2004 for a review),

¹Center for Astrophysics, University of Science and Technology of China, Hefei, Anhui, 230026, China

²Joint Institute of Galaxies and Cosmology, Shanghai Observatory and University of Science and Technology of China

³National Astronomical Observatories/Yunnan Observatory, Chinese Academy of Sciences, P.O. Box 110, Kunming, Yunnan 650011, China

⁴Department of Astronomy, University of Florida, Gainesville, FL 32611

and are generally believed to reside in most, if not all, galaxies with a spheroidal stellar component (Kormendy & Gebhardt 2001; Ferrarese & Ford 2005). However, little is known about their low mass counterparts, i.e. black holes with masses in the range of $10^3 - 10^6 M_\odot$, presumably in the centers of (dwarf) galaxies. These intermediate-mass black holes (IMBHs) may provide the ‘missing link’ in understanding the formation and evolution of SMBH seen today. In current models of galaxy evolution in a hierarchical cosmology, SMBH must have formed from much less massive “seed” black holes and grown up by accretion and/or merging. It is likely that there exists a population of IMBHs in the present universe, that have not the opportunity to be full-grown (e.g., Islam, Taylor & Silk 2004).

The search for IMBH turns out to be a difficult task, however, since IMBHs are beyond the reach of direct measurement using star/gas dynamics, by which most nearby SMBH are unveiled (see van der Marel 2004 for a review). The most promising approach is to search for dwarf active galactic nuclei (AGN) that are hosted in small galaxies—a scaled-down version of typical Seyfert galaxies and quasars. So far, convincing evidence for the existence of IMBHs has been found in only two AGN, NGC 4395 (Filippenko & Ho 2003, hereafter FH03; $M_{BH} = (3.6 \pm 1.1) \times 10^5 M_\odot$, Peterson et al. 2005, hereafter P05) and Pox 52 ($M_{BH} \approx 1.6 \times 10^5 M_\odot$, Barth et al. 2004, hereafter B04), with NGC 4395 being the only one having accurate black hole mass measurement via reverberation mapping. In addition, Greene & Ho (2004; hereafter GH04) found 19 IMBH candidates from the Sloan Digital Sky Survey (SDSS; Stoughton et al. 2002) First Data Release (Abazajian et al. 2003), whose black hole masses were estimated by using the linewidth-luminosity-mass scaling relationship (Kaspi et al. 2000). All these objects, except NGC 4395, have a very high accretion rate close to the Eddington limit.

In this paper, we report the discovery of a dwarf AGN with the estimated black hole mass as low as $\sim 10^5 M_\odot$, that is hosted by SDSS J160531.84+174826.1 (hereafter J1605+1748)—a dwarf (most likely disk) galaxy at a redshift $z = 0.032$. It was found from our on-going program of a systematic search for AGN with candidates IMBHs or hosted in dwarf galaxies from the SDSS Fifth Data Release. We assume a cosmology with $H_0=70 \text{ km s}^{-1} \text{ Mpc}^{-1}$, $\Omega_M=0.3$ and $\Omega_\Lambda=0.7$.

2. Data Analysis

2.1. Optical Spectrum

J1605+1748 was spectroscopically observed in the SDSS on June 12, 2005 with 4048s exposure and was classified as a galaxy by the SDSS pipeline. It has a redshift of $z = 0.03167$

as determined using the [O III] λ 5007 line. Figure 1 shows the rest frame spectrum with the Galactic reddening corrected ($E_{B-V} = 0.05$, Schlegel et al. 1998), which is dominated by starlight of the host galaxy. To subtract the starlight and the nuclear continuum, we followed our method¹ as described in detail in Zhou et al. (2006). The fit was good; the standard deviation of the distribution of the relative residuals $f_{residual}/f_{SDSS}$ in the emission line-free region around H α and H β is ≈ 0.05 , just the noise level with respect to the signal. The left-over emission line spectrum is plotted in Figure 1.

We fit the emission lines using the code described in detail in Dong et al. (2005). The peaks of the [N II] $\lambda\lambda$ 6548, 6583 doublet are well separated from the H α line, that shows an apparent broad component, owing to the relatively high S/N ratio ($\gtrsim 20$) in this spectral range and the narrowness of the lines. We model the [N II] doublet with two Gaussians with the line ratio $\lambda 6583/\lambda 6548$ fixed to the theoretical value 2.96. We use two Gaussians to model the narrow and broad components of H α , assuming the narrow component has the same profile and redshift as the [N II] doublet (see Zhou et al. 2006 for a full account of this assumption). A good fit is achieved, with a minimum reduced $\chi^2 = 0.73$ (d.o.f = 92), yielding a line width $794 \pm 42 \text{ km s}^{-1}$ FWHM for the broad H α component (see Figure 1). It has been noted by Véron-Cetty et al. (2001) that Lorentzian is a better profile to describe the broad lines in narrow line Seyfert 1s, that have FWHMs $< 2000 \text{ km s}^{-1}$. In view of this argument, we use a Lorentzian for the broad H α component and repeat the above fit; this yields a similarly good fit with reduced $\chi^2 = 0.71$ (d.o.f = 92), but a model over-predicted in the [N II] λ 6548 region by 7% of the [N II] λ 6548 peak height. So we adopt the Gaussian fit. To test the reliability of this broad H α component, we model the whole H α line with a single Gaussian with the center and width as free parameters; the result is unacceptable with a reduced $\chi^2 = 2.75$ (d.o.f = 95) and large residuals remained around H α . We therefore believe that the broad H α line is real. For the H β line, since its S/N ratio is relatively low (~ 10), we fix the profile parameters to those of H α , for both the narrow and broad components. For the [O III] $\lambda\lambda$ 4959, 5007 doublet, we only fit [O III] λ 5007 alone with one single Gaussian because [O III] λ 4959 is jaggy. We find the fit is good and no extended wing for [O III] λ 5007. We fit other narrow lines with a single Gaussian profile. The results of emission line fitting are listed in Table 1. The Balmer decrement is found to be 4.2 for the broad lines and 4.0 for the narrow lines, indicating an extinction color excess $E_{B-V} = 0.36$ and 0.31, respectively, assuming an intrinsic Balmer decrement of 3 (Dong et al. 2005, Zhou et al. 2006) and a SMC-like extinction curve. The ratios of the narrow lines

¹ Starlight is modeled with 6 spectral templates which were built up from the library of simple stellar populations of Bruzual & Charlot (2003) by using the Ensemble Learning Independent Component Analysis method (see Lu et al. 2006 for a detailed description).

$[\text{O III}]\lambda 5007/\text{H}\beta \gtrsim 3$ and $[\text{N II}]\lambda 6583/\text{H}\alpha \gtrsim 0.6$ place J1605+1748 into the AGN regime on the diagnostic diagram (Veilleux & Osterbrock 1987). It would be considered as a Seyfert 1.8 in the Osterbrock (1981) classification scheme, just like NGC 4395 (Filippenko & Sargent 1989, hereafter FS89) and POX 52 (B04).

2.2. Optical Image

We retrieved an archival HST image for J1605+1748, taken with the Wide Field Planetary Camera 2 (WFPC2) in June 1995 with a 500s exposure. The galaxy fell on the Wide Field camera ($0''.1/\text{pixel}$) as a “bonus” in an observation of Mkn 298 (Malkan et al. 1998). The F606W filter was used, which has a mean wavelength of 5947\AA and a FWHM of 1500\AA (1997 May WFPC2 SYNPHOT update). The data reduction was carried out following Malkan et al. (1998). On the HST image, galaxy is well resolved thanks to the superb spatial resolution. It is largely elongated with a major axis of about $6''$, and a bright, point-like nuclear source is evident. We perform structural decomposition using a “two-step” strategy: firstly fit to the one-dimensional surface brightness profile and then 2-D fitting to the image using the package GALFIT (Peng et al. 2002). We construct surface brightness models, for both the 1-D and 2-D cases, with a combination of different structural components: a point source represented by a point-spread function (PSF) that is generated with the Tiny Tim software (ver. 6.3)² for WFPC2; galactic component(s) parameterized by either an exponential or a Sérsic $r^{1/n}$ function (Sérsic 1968, see Graham & Driver 2005 for a concise review), or a combination of any of these two. We start off the fitting procedure with the simplest one-component model, and add in one more component only if the fit can be improved significantly by doing so. An additional constraint comes from the above optical spectral decomposition, which sets an upper limit on the contribution from a point source to be $\sim 15\%$ the total flux at 6000\AA .

Firstly, the azimuthally averaged 1-D radial profile of surface brightness is extracted using the IRAF ELLIPSE task. The best-fit model, which is plotted in Figure 2 along with the measured profile, is composed of a central point source plus two Sérsic components, one dominating the inner part of the galaxy and the other dominating the outer part. Leaving off the point source or one of the two Sérsic gives rise to unacceptable fits with significant and strongly structured residuals. The need for a central point source is not surprising, as revealed from the HST image (Figure 3). The presence of the second galactic component is found to be significant, as shown in Figure 2. Secondly, we perform 2-D image decomposition

²<http://www.stsci.edu/software/tinytim/>

using GALFIT, taking the results of the 1-D fits as initial values of the fitting parameters. The best-fit model turns out to be the same as for the 1-D fitting, but with somewhat different parameter values, especially for the central point source. We adopt the result from the 2-D fitting (Table 2) in this paper because 2-D modeling can recover a nuclear source much more reliable than 1-D fitting (Peng et al. 2002). Also displayed in Figure 3 are the images of the residuals and of the model components. The fit is good in general, with the standard deviation of the distribution for the fractional residuals $f_{residual}/f_{HST} \sim 0.1$ within the sky region 10 times or more brighter than the sky level. In comparison, other models with the same or less number of model components give rise to unacceptable fitting results that have much larger χ^2 and structures in the residuals.

For easy comparisons with NGC 4395 and POX 52, We derive the Johnson magnitudes from the F606W flux using the IRAF/SYNPHOT package. We assume a continuum similar to that of NGC 4395 ($f_\nu \propto \nu^{-1.5}$, Filippenko, Ho, & Sargent 1993) for the central point source, a template bulge spectrum (Kinney et al. 1996) for the inner Sérsic. We further make use of the SDSS spectrum (§2.1) for the outer Sérsic since it accounts for $\gtrsim 90$ per cent of the total F606W flux. The results are given in Table 2.

2.3. X-ray Data

As a remote member of the cluster Abell 2151, J1605+1748 was observed serendipitously several times by ROSAT and XMM-Newton. We retrieved from archives the observations with good effective exposures, one with the ROSAT Position Sensitive Proportional Counter (PSPC) in 1993, one with the ROSAT High Resolution Imager (HRI) in 1997, and one with the XMM-Newton EPIC-PN³ in 2003. X-ray data reduction were performed following the standard procedures, using the FTOOLS (ver. 6.1) utilities and the Science Analysis System (SAS, ver 6.0.0) for ROSAT and XMM-Newton data, respectively. Table 3 lists some relevant parameters for the X-ray observations and data reduction. For the XMM-Newton data, exposure periods which suffered from high flaring background caused by soft protons are removed. Source counts are extracted from a circle (see Table 3) and background events are extracted from source-free regions using a concentric annulus for PSPC and HRI, and two circles at the same CCD read-out column as the source position for PN. In each of these observations an X-ray source was detected at the $\gtrsim 6\sigma$ significance levels at a position coincident with the optical point source of the galaxy within one σ positional error. The position of the X-ray source detected with XMM-Newton is RA=16:05:31.87, Dec=17:48:26.11

³The source position falls into a gap between CCD chips on the two EPIC-MOS detectors.

(J2000), with an error circle of $0''.9$ (1σ) in radius.

The spectral fitting is carried out using XSPEC (ver. 12.2.1). Due to the small number of source counts, 58 for PSPC (0.1–2.4 keV) and 79 for PN (0.3–8keV), the spectra are rebinned to have a minimum of 6 counts in each energy bin, and the Cash-statistic is adopted in the minimization instead of χ^2 . We fit simultaneously the two spectra assuming the same spectral models with the parameters tied together except the normalizations. The spectra can be fitted with a power law with a photon index $\Gamma = 2.1 \pm 0.3$ and an absorption column density close to the Galactic value ($3.5 \times 10^{20} \text{cm}^{-2}$). The unabsorbed 2–10 keV flux is $3.0 \times 10^{-14} \text{ ergs s}^{-1} \text{ cm}^{-2}$ measured by XMM-Newton, corresponding to a luminosity of $7.0 \times 10^{40} \text{ ergs s}^{-1}$. The best fit normalization at 1 keV is a factor of 2 higher for ROSAT than for XMM-Newton. To test the significance of this variation, we search for the maximum confidence contours in the parameter space of the two normalizations (two free parameters) within which they differ from each other; we find that the variation is marginally significant at the $\sim 90\%$ level. The HRI flux is found to be roughly consistent with the XMM-Newton value assuming the same spectral shape.

3. Results and Discussion

In summary, observations of J1605+1748 reveal the presence of an optical bright point source based on its HST image, a broad $\text{H}\alpha$ component with FWHM 781 km s^{-1} (after correction for the instrumental broadening of 141 km s^{-1} FWHM) and AGN-like narrow emission line ratios, a non-thermal X-ray luminosity ($7.0 \times 10^{40} \text{ ergs s}^{-1}$ in 2–10 keV) and possible X-ray variability. All these observational facts point to the presence of a Seyfert 1 type dwarf active nucleus in J1605+1748. This can be further supported by the striking similarities between J1605+1748 and the two well known dwarf AGN NGC 4395 and POX 52, whose properties are summarized in Table 4. In fact, the AGN in J1605+1748 lies in between NGC 4395 and POX 52 in terms of the observed luminosities of both $\text{H}\alpha$ and optical continuum. Furthermore, J1605+1748 is more luminous at hard X-rays than NGC 4395 (no data available for POX 52 so far). The equivalent width of its broad $\text{H}\beta$ component ($\sim 20\text{\AA}$, relative to the nuclear continuum calculated from the HST F606W flux of the point source) is typical of Seyfert 1.8/1.9 nuclei and similar to that of NGC 4395 (FS89).

We estimate the mass of its central black hole following the widely used linewidth-luminosity-mass scaling relation (e.g., Vestergaard 2002; McLure & Jarvis 2002; GH04). The intrinsic monochromatic luminosity at 5100\AA is estimated to be $L_{5100} \equiv \lambda L_{\lambda}(5100\text{\AA}) = 4.0 \times 10^{41} \text{ ergs s}^{-1}$ from the $\text{H}\alpha$ luminosity using the $L_{\text{H}\alpha} - L_{5100}$ relation given by Greene & Ho

(2005)⁴, incorporating the extinction correction that is derived from the Balmer decrement for the broad lines (§2.1). Using Equation (6) in Greene & Ho (2005), we find a black hole mass $6.9 \times 10^4 M_\odot$. The uncertainty of the black hole mass thus estimated is not well understood, however. As pointed out by Vestergaard & Peterson (2006), the statistical accuracy of the masses from such a scaling relationship is a factor of ~ 4 (1σ), and, for individual mass estimates, the uncertainty can be as large as an order-of-magnitude. Using the BLR-size–luminosity relations from Kaspi et al. (2005) and Bentz et al. (2006), we find a black hole mass of $5.8 \times 10^4, 2.6 \times 10^5 M_\odot$, respectively; here we adopt the formalism and scale factor from Peterson et al. (2004) and Onken et al. (2004), with $L_{5100} = 4.0 \times 10^{41}$ ergs s^{-1} , $\sigma_{\text{line}} = 332$ km s^{-1} estimated from the broad H α component.

Assuming a spectral energy distribution (SED) similar to that of NGC 4395, the bolometric luminosity L_{bol} for J1605+1748 is estimated to be $\approx 3.7 \times 10^{42}$ ergs s^{-1} by scaling their L_{5100} luminosities using the NGC 4395 data in P05. This is consistent with the bolometric correction $L_{\text{bol}} \approx 9L_{5100}$ used for normal QSOs (Kaspi et al. 2000). Then, the Eddington ratio $L_{\text{bol}}/L_{\text{Edd}}$ is ≈ 0.3 for a black hole mass of $6.9 \times 10^4 M_\odot$. This indicates that J1605+1748 is at a high accretion state, similar to POX 52. The broad-band spectral index $\alpha_{\text{ox}} \equiv -0.3838 \log[F_\nu(2 \text{ keV})/F_\nu(2500 \text{ \AA})] \simeq -1.1$ agrees well with the extrapolation down to low luminosity of the α_{ox} –luminosity relation given by Strateva et al. (2005, see also Yuan Brinkmann & Siebert 1998) for radio-quiet AGNs, similar to the result for a small sample of IMBH AGN (Greene & Ho 2006).

As results from the above HST image decomposition analysis (§2.2), the galaxy is composed of three components, a central point source as the AGN, an inner Sérsic with $r_e = 0''.18$ (114 pc), and an outer Sérsic with $r_e = 1''.58$ (1 kpc), which account for 6.0, 2.6, 91.4 per cent of the total F606W light, respectively. We tend to identify the outer Sérsic to be a galactic disk, because of 1) its exponential-like radial profile with the Sérsic index $n = 0.8$, close to 1 for exponential⁵, 2) the disk-like isophote shape ($c = -0.1$), 3) the apparent extreme flattening (Hubble type E6.3 based on the axis ratio), that is very unlikely for an elliptical (Binney & de Vaucouleurs 1981), and particularly, 4) the existence of the additional inner Sérsic component.

With an effective radius of $0''.18$, the inner Sérsic is merely resolved by the Wide Field Camera; however, fits without this component result in large residuals and an over-predicted

⁴This value is well consistent with that estimated using the HST F606W flux of the point source assuming a power-law spectrum ($f_\lambda \propto \lambda^{-\alpha_\lambda}$), $(3.5 - 4.6) \times 10^{41}$ ergs s^{-1} for $\alpha_\lambda = 0 - 2$.

⁵This somewhat shallower inner profile may be caused by dust extinction in the disk, which is indicated by the Balmer decrements, since the extinction aggravates inwards for an inclined disk ($i = \cos^{-1}(b/a) = 66^\circ$).

point source, as displayed in Figure 2. Its size is too large for being a nuclear star cluster. The fitted image has a boxy shape ($c = 0.6$) and a rather flat profile ($n = 0.4$), suggesting a box-/peanut-shaped bulge or an edge-on *nuclear* bar—their presence in disk galaxies are known for many years (eg. Burbidge & Burbidge 1959; Evans 1951; de Vaucouleurs 1975). We prefer the nuclear bar speculation because there is a $\sim 17^\circ$ mis-alignment between its major axis and that of the disk, that is more natural for the bar scenario; moreover, a bar can provide an efficient mechanism of fueling gas to the AGN but a bulge cannot (e.g., Shlosman et al. 1989). In fact, a boxy bulge may evolve from a bar, or may simply be (part of) a bar viewed edge-on (see Kormendy & Kennicutt 2004 for a review). Regardless of its nature, we predict the mass of the central black hole based on the empirical $M_{BH} - L_{bul}$ correlations using the absolute magnitudes (Table 3, corrected for the internal extinction $E_{B-V} = 0.36$). Using the formalism from Marconi & Hunt (2003) and McLure & Dunlop (2002), we find 2.5×10^5 and $2.6 \times 10^4 M_\odot$, respectively, roughly consistent with our estimate from the scaling relation considering the large uncertainties. Furthermore, following the empirical relation between M_{BH} and bulge concentration (Graham et al. 2001, Graham et al. 2003), we obtain $M_{BH} = 1.6 \times 10^5 M_\odot$, also consistent with the virial mass estimate. Either bars or boxy bulges (as a kind of “pseudobulges” [Kormendy 1993]) form out of disk material (Kormendy & Kennicutt 2004). So, probably just as stated by Carollo (2004), “the requirement for making a supermassive central black hole is that the galaxy is capable of reaching sufficiently high central baryonic densities.”

This work is supported by Chinese NSF grants NSF-10533050 and NSF-10573015. XBD is partially supported by a postdoc grant from Wang Kuan-Cheng Foundation. We wish to thank the anonymous referee for constructive comments and suggestions, and thank Alister Graham for helpful comments. XBD thank Professor Robert Kennicutt, Jr. for valuable suggestions and insightful discussions during his visit to USTC this summer, and thank Professor Zhenlong Zou for helpful comments and suggestions. Funding for the Sloan Digital Sky Survey (SDSS)⁶ has been provided by the Alfred P. Sloan Foundation, the Participating Institutions, the National Aeronautics and Space Administration, the National Science Foundation, the U.S. Department of Energy, the Japanese Monbukagakusho, and the Max Planck Society. The SDSS is managed by the Astrophysical Research Consortium (ARC) for the Participating Institutions.

⁶ The SDSS Web site is <http://www.sdss.org/>.

REFERENCES

- Abazajian, K., et al. 2003, *AJ*, 126, 2081
- Barth, A. J., Ho, L. C., Rutledge, R. E., & Sargent, W. L. W. 2004, *ApJ*, 607, 90 (B04)
- Bentz, M. C., Peterson, B. M., Pogge, R. W., Vestergaard, M., & Onken, C. A. 2006, *ApJ*, 644, 133
- Binney, J., & de Vaucouleurs, G. 1981, *MNRAS*, 194, 679
- Bruzual, G., & Charlot, S. 2003, *MNRAS*, 344, 1000
- Burbidge, E. M., & Burbidge, G. R. 1959, *ApJ*, 130, 20
- Carollo, C. M. 2004, *Coevolution of Black Holes and Galaxies*, p. 231 (astro-ph/0306021)
- de Vaucouleurs, G. 1975, *ApJS*, 29, 193
- Dong, X.-B., Zhou, H.-Y., Wang, T.-G., Wang, J.-X., Li, C., & Zhou, Y.-Y. 2005, *ApJ*, 620, 629
- Evans, D. S. 1951, *MNRAS*, 111, 526
- Ferrarese, L., & Ford, H. 2005, *Space Science Reviews*, 116, 523
- Filippenko, A. V., & Ho, L. C. 2003, *ApJ*, 588, L13
- Filippenko, A. V., Ho, L. C., & Sargent, W. L. W. 1993, *ApJ*, 410, L75
- Filippenko, A. V. & Sargent, W. L. W. 1989, *ApJ*, 342, L11 (FS89)
- Graham, A. W., Erwin, P., Caon, N., & Trujillo, I. 2001, *ApJ*, 563, L11
- Graham, A. W., Erwin, P., Caon, N., & Trujillo, I. 2003, *Revista Mexicana de Astronomia y Astrofisica Conference Series*, 17, 196
- Graham, A. W., & Driver, S. P. 2005, *Publications of the Astronomical Society of Australia*, 22, 118
- Greene, J. E., & Ho, L. C. 2004, *ApJ*, 610, 722 (GH04)
- Greene, J. E., & Ho, L. C. 2005, *ApJ*, 630, 122
- Greene, J. E., & Ho, L. C. 2006, *ArXiv Astrophysics e-prints*, arXiv:astro-ph/0608061

- Islam, R. R., Taylor, J. E., & Silk, J. 2004, MNRAS, 354, 427
- Kaspi, S., Smith, P. S., Netzer, H., Maoz, D., Jannuzi, B. T., & Giveon, U. 2000, ApJ, 533, 631
- Kaspi, S., Maoz, D., Netzer, H., Peterson, B. M., Vestergaard, M., & Jannuzi, B. T. 2005, ApJ, 629, 61
- Kinney, A. L., Calzetti, D., Bohlin, R. C., McQuade, K., Storchi-Bergmann, T., & Schmitt, H. R. 1996, ApJ, 467, 38
- Kormendy, J. 1993, IAU Symp. 153: Galactic Bulges, 153, 209
- Kormendy, J. & Gebhardt, K. 2001, in 20th Texas Symposium on Relativistic Astrophysics, ed. J. C. Wheeler & H. Martel (Melville, NY: American Institute of Physics), 363
- Kormendy, J. 2004, Coevolution of Black Holes and Galaxies, p. 1 (astro-ph/0306353)
- Kormendy, J., & Kennicutt, R. C., Jr. 2004, ARA&A, 42, 603
- Lu, H., Zhou, H., Wang, J., Wang, T., Dong, X., Zhuang, Z., & Li, C. 2006, AJ, 131, 790
- Malkan, M. A., Gorjian, V., & Tam, R. 1998, ApJS, 117, 25
- Marconi, A. & Hunt, L. K. 2003, ApJ, 589, L21
- McLure, R. J., & Jarvis, M. J. 2002, MNRAS, 337, 109
- Moran, E. C., Filippenko, A. V., Ho, L. C., Shields, J. C., Belloni, T., Comastri, A., Snowden, S. L., & Sramek, R. A. 1999, PASP, 111, 801
- Onken, C. A., Ferrarese, L., Merritt, D., Peterson, B. M., Pogge, R. W., Vestergaard, M., & Wandel, A. 2004, ApJ, 615, 645
- Osterbrock, D. E. 1981, ApJ, 249, 462
- Peng, C. Y., Ho, L. C., Impey, C. D., & Rix, H.-W. 2002, AJ, 124, 266
- Peterson, B. M., et al. 2004, ApJ, 613, 682
- Peterson, B. M., et al. 2005, ApJ, 632, 799 (P05)
- Schlegel, D. J., Finkbeiner, D. P., & Davis, M. 1998, ApJ, 500, 525
- Sérsic, J. L. 1968, Atlas de Galaxias Australes (Córdoba: Obs. Astron., Univ. Nac. Córdoba)

- Shlosman, I., Frank, J., & Begelman, M. C. 1989, *Nature*, 338, 45
- Stoughton, C. et al. 2002, *AJ*, 123, 485
- Strateva, I. V., Brandt, W. N., Schneider, D. P., Vanden Berk, D. G., & Vignali, C. 2005, *AJ*, 130, 387
- van der Marel, R. P. 2004, *Coevolution of Black Holes and Galaxies*, p. 37 (astro-ph/0302101)
- Vestergaard, M. 2002, *ApJ*, 571, 733
- Vestergaard, M., & Peterson, B. M. 2006, *ApJ*, 641, 689
- Vaughan, S., Iwasawa, K., Fabian, A. C., & Hayashida, K. 2005, *MNRAS*, 356, 524
- Veilleux, S., & Osterbrock, D. E. 1987, *ApJS*, 63, 295
- Véron-Cetty, M.-P., Véron, P., & Gonçalves, A. C. 2001, *A&A*, 372, 730
- Vestergaard, M. 2002, *ApJ*, 571, 733
- Yuan, W., Brinkmann, W., Siebert, J., & Voges, W. 1998, *A&A*, 330, 108
- Zhou, H., Wang, T., Yuan, W., Lu, H., Dong, X., Wang, J., & Lu, Y. 2006, *ApJS*, 166, 128

Table 1. Fitted emission line parameters

Line	Centroid ^a	FWHM ^b	Flux ^c
[O II] λ 3727	3728.47 ± 0.51	281 ± 102	28.0 ± 8.5
H β (narrow) ^d	4862.14 ± 0.24	137	17.0 ± 2.9
H β (broad) ^e	4860.93 ± 1.26	781	27.3 ± 5.8
[O III] λ 5007	5008.25 ± 0.08	160 ± 12	53.7 ± 2.8
[O I] λ 6301	6302.83 ± 0.86	277 ± 84	9.3 ± 2.6
H α (narrow)	6564.53 ± 0.06	137 ± 8	67.3 ± 4.1
H α (broad)	6565.78 ± 0.30	781 ± 42	115.2 ± 5.3
[N II] λ 6583 ^d	6585.22	137	38.4 ± 1.9
[S II] λ 6716	6718.43 ± 0.18	142 ± 20	18.2 ± 1.9
[S II] λ 6731 ^f	6732.81	142	14.6 ± 1.9

Note. — (a): Vacuum rest-frame wavelengths, in unit of Å. (b): Corrected for the instrumental broadening; in unit of km s⁻¹. (c): In unit of 10⁻¹⁷ergs s⁻¹ cm⁻². (d): Adopting the profile of narrow H α . (e): Adopting the profile of broad H α . (f): Adopting the profile of [S II] λ 6716.

Table 2. Two-Dimensional Image Fitting Parameters

Func.	m_{606}^a	M_R^a	M_B^a	r_e	n	b/a	PA	c	notes
(1)	(2)	(3)	(4)	(5)	(6)	(7)	(8)	(9)	(10)
PSF	21.1	-14.6	-14.6	–	–	–	–	–	AGN
Sérsic	21.9	-13.9	-12.4	0.18	0.4	0.28	82	+0.6	Bar?
Sérsic	18.1	-17.8 ^b	-16.4	1.58	0.8	0.37	65	-0.1	Disk

Note. — Col. (1): Components used in the fit. Col. (2): The F606W integrated magnitudes on the Vega system. Col. (3): The absolute Johnson R magnitudes. Col. (4): The absolute Johnson B magnitudes. Col. (5): The effective radius of the Sérsic law, in arcsecond. Col. (6): The Sérsic exponent. Col. (7): Axis ratio. Col. (8): Position angle, in degree. Col. (9): Diskiness (negative)/boxiness (positive) parameter, defined in equation (3) of Peng et al. (2002). (a): All the magnitudes are corrected for the Galactic extinction; see the text for the transformation from mag_{606} to Johnson B and V magnitudes. (b): In good agreement with the SDSS r -band absolute magnitude derived from the fit with an exponential model, $M_r = -17.8$.

Table 3. X-ray observations and data reduction information

	XMM/EPIC-PN	ROSAT/HRI	ROSAT/PSPC
Obs. id	0147210301	RH703861A01	RP800517N00
good exposure	5.7ks	54.9ks	12.1ks
$R_{\text{source extraction}}$	30''	25''	45''
net count rate*	1.2 ± 0.2	0.12 ± 0.02	0.35 ± 0.08
flux*	3.4 ± 0.6	4.2 ± 0.7	7.1 ± 1.4

Note. — (*): Measured in the 0.3–2.4keV range; count rate in unit of 10^{-2}cts s^{-1} , and flux (without Galactic absorption correction), $10^{-14}\text{ergs s}^{-1} \text{cm}^{-2}$.

Table 4. Comparison with NGC 4395 and POX 52

Object (1)	M_B^{Host} (2)	M_B^{AGN} (3)	$L_{H\alpha}^{br}$ (4)	$L_{X,Soft}$ (5)	$L_{X,Hard}$ (6)
NGC 4395	−17.5 ^a	−10.8 ^a	1.2 ^b	1.3 ^c	1.5 ^d
J1605+1748	−16.4	−14.6	27	1100 ^e	7.0
POX 52	−16.8 ^f	−16.7 ^f	120 ^f	–	–

Note. — Col. (4, 5): In unit of 10^{38} ergs s^{-1} . Col. (6): Unabsorbed X-ray luminosity in the 2 – 10keV range, in unit of 10^{40} ergs s^{-1} . (a): From FH03. (b): From FS89. (c): Observed X-ray luminosity in the 0.2 – 2keV range from Moran et al. 1999. (d): From Vaughan et al. 2005. (e): Mean observed X-ray luminosity in the 0.3 – 2.4keV. (f): Form B04.

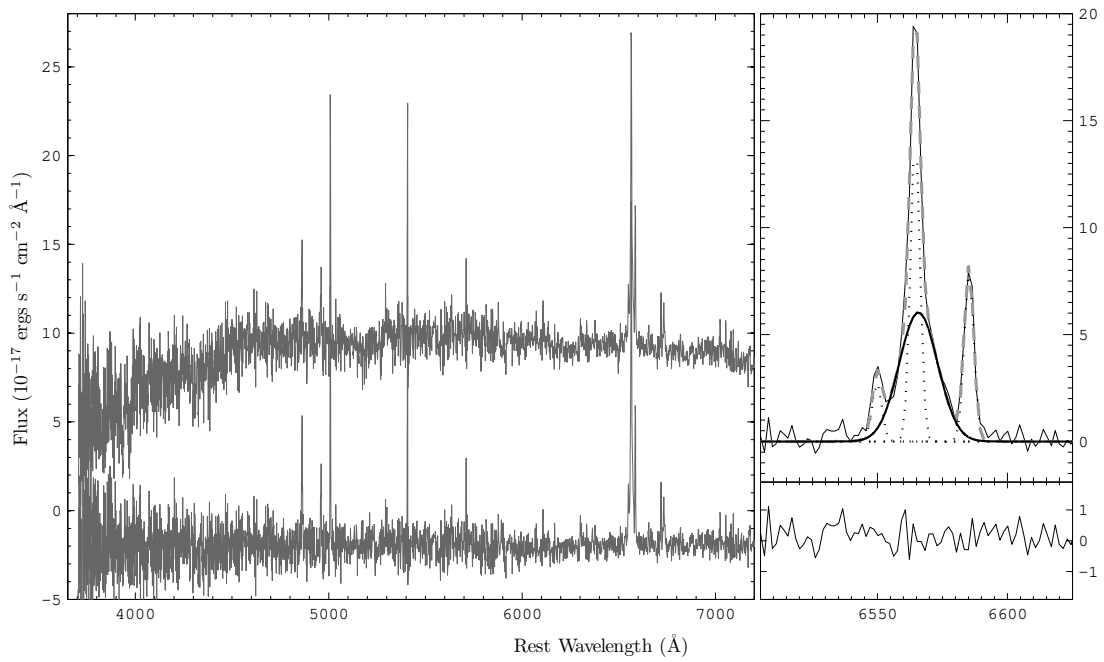


Fig. 1.— SDSS spectrum and the line fit. Left: The SDSS spectrum (top) and the starlight/continuum subtracted residual (bottom, offset downward by 2 units for clarity). Right: The line decomposition in the $H\alpha+[N II]$ region. The upper panel shows the original data (thin solid line), the fitted narrow lines (dotted lines), the fitted broad $H\alpha$ (thick solid line) and the sum of the fit (gray dashed line). The lower panel, the residual of the fit.

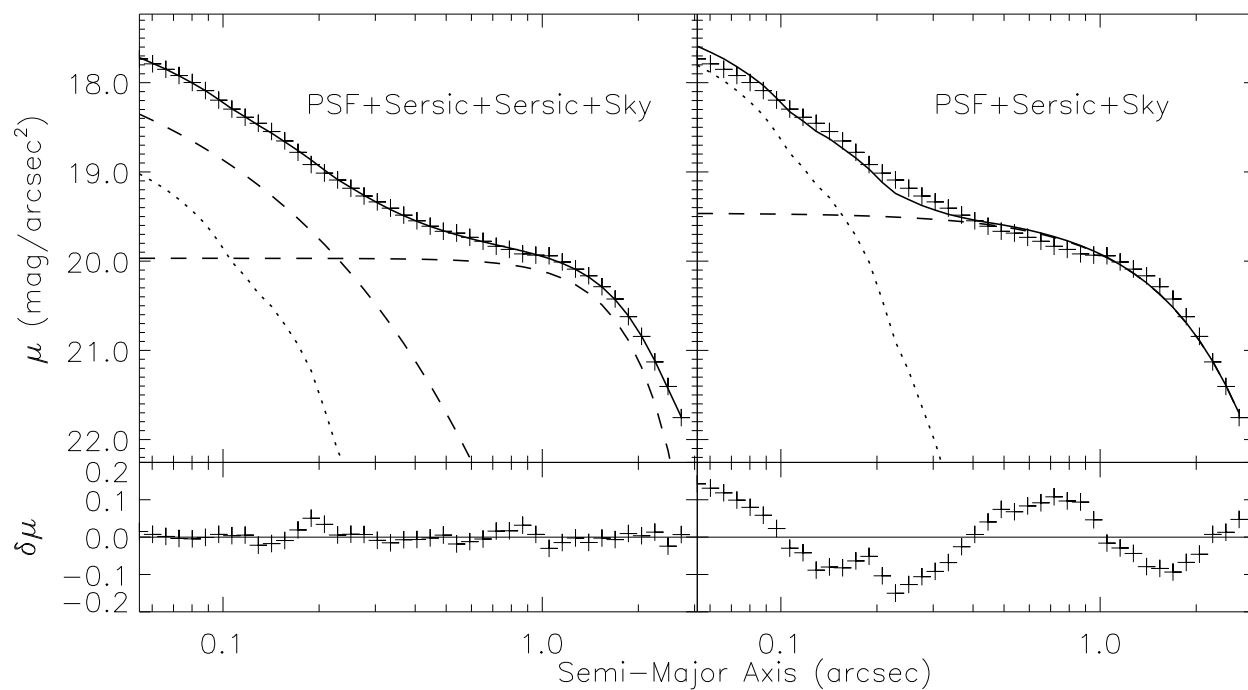


Fig. 2.— One dimensional fitting of the radial profile, with PSF + two Sérsic model (left panel) and PSF + a Sérsic model (right panel). Each panel shows the point-source component (dotted), the host-galaxy component(s) (dashed), and the sum (solid). Residuals are also displayed in the bottom. As indicated in the right panel, fit with only one Sérsic for the host galaxy yields large residuals left and an over-predicted point source component. The results of the 1-D fits are taken as initial values of the fitting parameters of the subsequent 2-D decomposition.

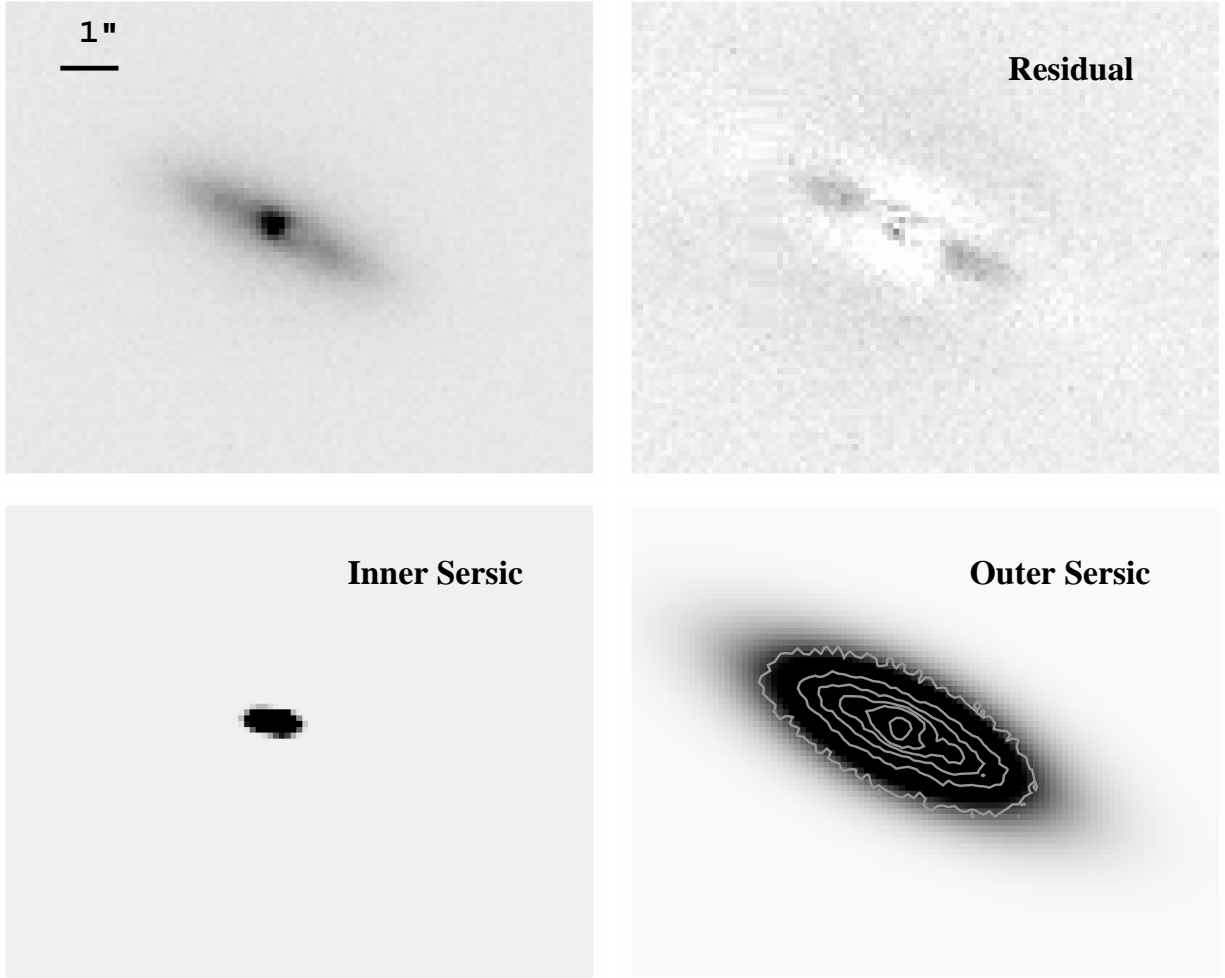


Fig. 3.— Two-dimensional decomposition of the HST/WFPC2 F606W image. Top: the original data (left) and the residual from the best-fitting PSF + two Sérsic model (right). The standard deviation of the distribution for the fractional residuals $f_{residual}/f_{HST} \sim 0.1$ within the sky region 10 times or more brighter than the sky level. Bottom: the best-fit inner Sérsic component (left) and outer Sérsic component with the contours of the original image overlaid (right). Images have the same size.

Supplementary information:

[See more at <http://staff.ustc.edu.cn/~xbdong/J1605+1748/>]

Dwarf Disk Galaxy with an IMBH

J160531.84+174826.1 : $B=-16.4$, $R=-17.8$

$z=0.032$

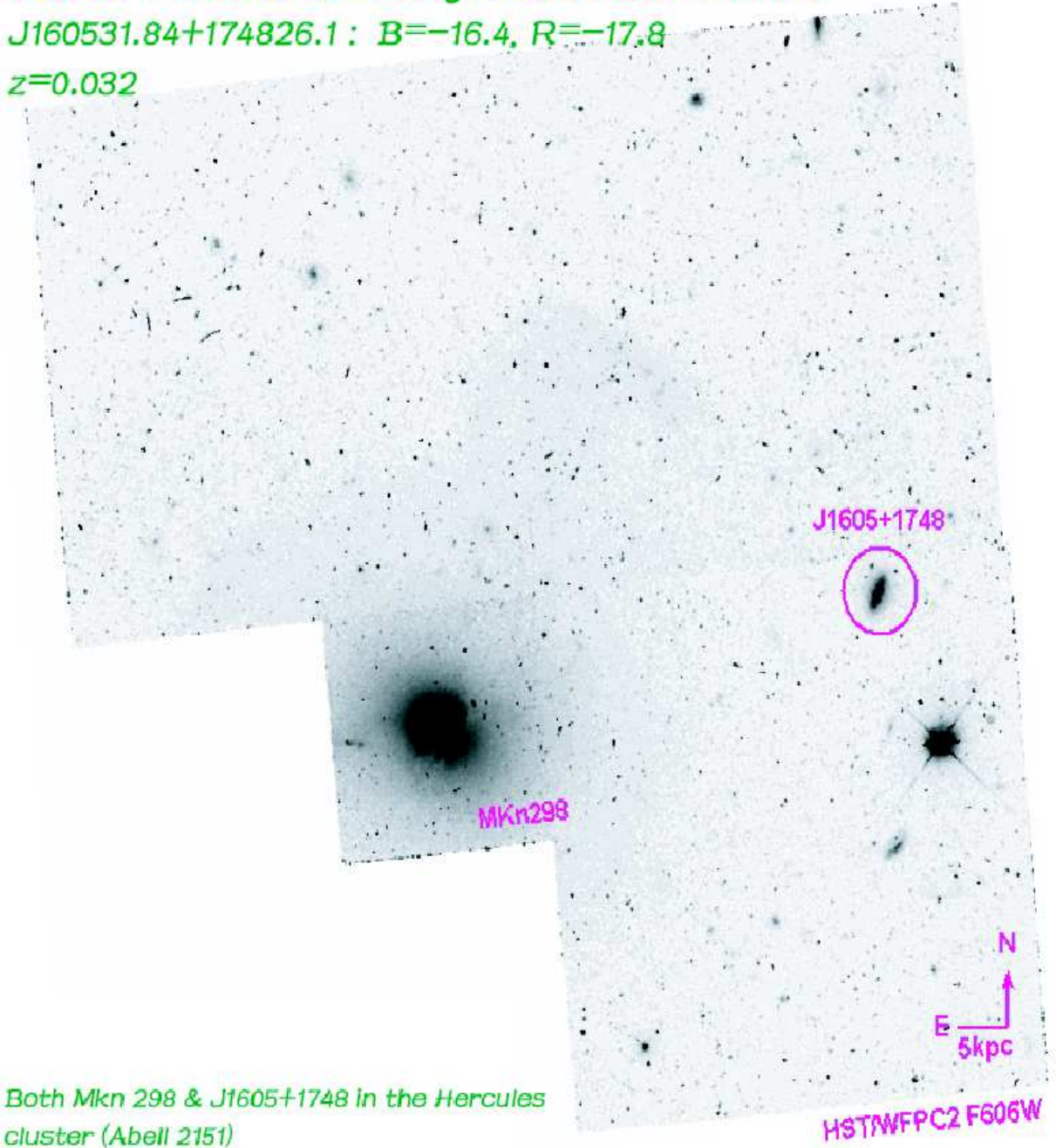


Fig. 4.— HST/WFPC2 F606W preview image for J1605+1748 and its neighbor Mkn 298. They are in the Hercules cluster (Abell 2151). Displayed with a logarithmic stretch.